ELSEVIER

Journal of Chromatography A, 845 (1999) 303–316

JOURNAL OF CHROMATOGRAPHY A

Continuous split flow-thin cell fractionation of starch particles

Catia Contado*, Filomena Riello, Gabriella Blo, Francesco Dondi

Department of Chemistry, University of Ferrara, Via L. Borsari 46, I-44100 Ferrara, Italy

Abstract

The fractionation of starch granules was investigated using a SPLITT (split flow-thin) cell, a relatively new system for fast, continuous binary separations. The effect of such basic separation parameters as carrier composition, relative flow-rates and sample concentration on the SPLITT cell performance were exploited. The obtained starch fractions were checked by both optical microscopy and sedimentation/steric field flow fractionation (Sd/StFFF). The sedimentation field flow fractionation technique was employed for the starch sample using the density compensation procedure. © 1999 Elsevier Science B.V. All rights reserved.

Keywords: Split flow-thin cell fractionation; Field flow fractionation; Starch; Polysaccharides

1. Introduction

Starch is one of the most abundant polysaccharides in nature and is isolated in the form of granules. Its great economic relevance for industry is well known and, indeed, granule size is a contributing factor in the quality of many starch products [1]. Microscopically, the granules range from 1 to 55 μm in diameter depending on the kind of starch, granule density being around 1.5 g/ml. This high density and the granular structure facilitates starch separation by centrifugation/gravity sedimentation or by filtration during isolation, chemical modifications and washing [2].

In response to industrial demand for well characterized starch granules, the classical sedimentation and centrifugation techniques are commonly used for both granule fractionation and size characterization [3]. However, these techniques give low resolution, are time consuming and discontinuous in separation practice.

In the present work a SPLITT (split flow-thin) cell – a relatively new class of thin flow-cell techniques still under development [4] – is tested as a continuous, fast and tunable preparatory tool in the separation of different dimensional fractions of a wheat starch sample. A SPLITT fractionation (SF) system employing gravitational force is illustrated in Fig. 1. For particles of starch larger than 1 μm, a gravitational field provides good separation. Use of a SF system proves advantageous for many analytical [5–7] and preparative [8,9] applications because it is fast, simple, theoretically tractable, provides high resolution and gentle, continuous processing on a relatively inexpensive infrastructure. When scaled up, it is envisioned that this technique will provide an effective sample preparation tool for processing industrial [8–10], environmental [11] and biological samples [12–15] at sample throughput rates ranging from a few grams to several kilograms per hour.

In order to more accurately describe the SPLITT separation results in terms of particle size distribution, sedimentation/steric field flow fractionation (Sd/StFFF) was used in addition to optical microscopy. In the former approach, starch samples were

*Corresponding author.
E-mail address: kat@dns.unife.it (C. Contado)

0021-9673/99/$ – see front matter
PII: S0021-9673(99)00231-9

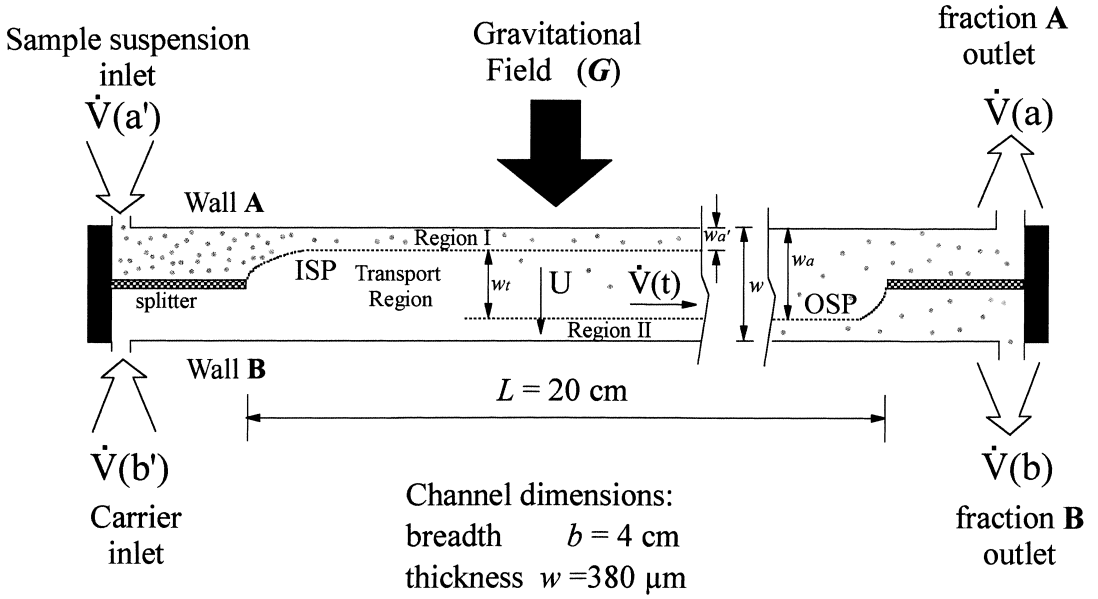

Fig. 1. SPLITT cell – side view.

analyzed by Sd/StFFF using the previously consolidated density compensation procedure [16,17]. Sd/StFFF has elsewhere been applied for the size characterization of starch samples, the difference here being that it is coupled with the SPLITT cell thus making it possible to collect much more integrated information from these two complementary separation techniques: the latter a preparation tool, the former working on analytical scale. Together, they can give good, quick, inexpensive information over a broader size range, thanks to their easy experimental feasibility.

In this first work on SPLITT-Sd/StFFF separation and characterization of starch granules several operating conditions were investigated, i.e., the effect of carrier composition, relative flow-rates and inlet sample concentration. Three kinds of mobile phases, four different feed sample concentrations and a combination of six inlet flow-rates were tested for a single cut sample. This first study has made it possible to define an initial set of practical separation conditions for the fractionation of starch granules and will provide the basis for further studies (e.g., quantitative analyses).

2. Theory

The SPLITT fractionation theory has been presented in numerous publications [8,18]. The separation is performed inside a thin channel, where the behavior of a sample particle depends on the balance between gravitational and frictional forces, combined with the action of the fluxes operative within the cell.

A side view of the SPLITT cell used in this study is illustrated in Fig. 1. The sample suspended in a suitable carrier fluid is continuously introduced through the top inlet at a predetermined volumetric flow-rate $\dot{V}(a')$. At the same time, pure carrier fluid enters through the bottom inlet at a flow-rate $\dot{V}(b')$; where the two inlet streams join to form a single stream we have what is called the inlet splitting plane (ISP). When the fluid stream reaches the end of the channel, it is mechanically divided into two fractions by an outlet splitter. The slower settling particles emerge from the upper outlet at a flow-rate $\dot{V}(a)$ while those that settle faster exit the lower outlet at a flow-rate $\dot{V}(b)$. Analogously to what has just been defined, the outlet splitting plane separates the two fluid elements eluting from a and b. In this way

the splitting planes divide the channel volume into distinct laminae [14].

The total volumetric flow-rate $\dot{V}$ in the channel can be written in several equivalent forms, for example as the sum of the flow-rates of constituent laminae [15]:

$$\dot{V} = \dot{V}(a') + \dot{V}(b') = \dot{V}(a) + \dot{V}(b) = \dot{V}(a') + \dot{V}(t) + \dot{V}(b) \quad (1)$$

where $\dot{V}(t)$ is the fluid flow proceeding in the transport layer. This flow-rate can be obtained from Eq. 1 as:

$$\dot{V}(t) = \dot{V}(a) - \dot{V}(a') = \dot{V}(b') - \dot{V}(b) \quad (2)$$

By assuming that, during their residence in the SPLITT cell, the particles are driven from wall A to wall B at constant velocity U, the volumetric flow-rate $\Delta\dot{V}$ of the lamina traversed by a compact spherical particle is simply given by [18]:

$$\Delta\dot{V} = bLU = \frac{bLGd^2|\Delta\rho|}{18\eta} \quad (3)$$

which contains the physical dimensions of the channel: b is the width and L the length; U, the sedimentation velocity of the particle, can be made explicit in terms of G the acceleration of gravity, d the particle diameter, $\Delta\rho$ the difference between particle density ρ_p and carrier density ρ_l and η the viscosity of the carrier. $\Delta\dot{V}$ must thus be interpreted as a hypothetical volumetric flow-rate, connected to the sedimentation velocity U.

Of critical importance are the relative values of $\Delta\dot{V}$ and $\dot{V}(t)$, indicating whether particles exit the channel through outlet a or b. For a sample introduced close to the ISP, particles exit from outlet a if:

$$\Delta\dot{V} \leq \dot{V}(t) \quad (4)$$

and from outlet b if:

$$\Delta\dot{V} > \dot{V}(t) \quad (5)$$

The diameter at which 50% of the particles exit outlet b is called the cut-off diameter d_c, expressed as [19,20]:

$$d_c = \sqrt{\frac{18\eta[\dot{V}(a) - 0.5\dot{V}(a')]}{bL(\rho_p - \rho_l)G}} \quad (6)$$

Once d_c has been chosen for a given channel, the difference between $\dot{V}(a)$ and $0.5\dot{V}(a')$ is set according to Eq. 6. However, the four constituents flow-rates $\dot{V}(a)$, $\dot{V}(a')$, $\dot{V}(b)$, $\dot{V}(b')$ are not uniquely defined by this equation. Some criteria useful for setting the flow-rates are given in a paper on the optimization of SPLITT operations [21]. For maximum resolution, the ratio between $\dot{V}(a')/\dot{V}(t)$ and $\dot{V}(b')/\dot{V}(t)$ are chosen most often within 0.1–0.3 and 1.5–3.0, respectively [7]. A separation can be successfully carried out if the difference between the diameters of the particles exiting from a (d_0) and b (d_1) is small. The particles falling between these two sizes (d_1 and d_0), which are not fully resolved, exit from both outlets in different portions. Separation resolution in the SF system can be related to channel flow-rates defining an index which measures the relative breadth of the unresolved region. It has been demonstrated that for sedimentation particles the equation of the resolving power has the following form [21]:

$$\frac{d_1}{\Delta d} = \frac{d_1}{d_1 - d_0} \cong 2\frac{\dot{V}(a)}{\dot{V}(a')} \quad (7)$$

According to Eq. 7 the ratio of $\dot{V}(a)$ to $\dot{V}(a')$ allows control of the range of unresolved particles which exit both outlets a and b.

The high resolution in the operative transport mode is contingent on compression of the feed substream a′ into a thin lamina near wall A, and the sharpness of the separation, as in chromatography, can be judged by the number N of the theoretical plates generated during transport. For field-driven (SPLITT) migration, the effective N is given by the ratio of two energies [21]:

$$N = \frac{Fw_t}{2kT} = \frac{\pi d^3 \Delta\rho G w_t}{12kT} \quad (8)$$

where F is the force on the particle inducing its transport, w_t the length of the transport path, and kT the thermal energy. Generally $N \geq 10^2$ values are required to assure achievable resolution, and each type of macromolecule or particle should be checked against this criterion.

Size distribution data can be obtained applying the SdFFF technique to samples fractionated by SPLITT cell in the steric mode. For steric FFF techniques, including Sd/StFFF, the relationship between retention time t_R and particle diameter d must be empirically established by a calibration procedure. Such calibration is needed because the behavior of the relatively large (over 1 μm in diameter) particles subjected to steric FFF is substantially influenced by hydrodynamic effects, particularly by hydrodynamic lift forces tending to drive them away from the wall where they would normally accumulate [22].

The calibration is obtained by plotting the log t_R for a series of polystyrene latex particles of known diameter versus their correspondent log d; the linear plot is:

$$\log t_R = -S_{ds}\log d + (S_{\Delta\rho}\log G\Delta\rho + \log t_{R1}) \quad (9)$$

where S_{ds} is the diameter-based selectivity, defined as:

$$S_{ds} = \left|\frac{\mathrm{d}\log t_R}{\mathrm{d}\log d}\right| \quad (10)$$

with a value typically around 0.75 [23]. The parameter $S_{\Delta\rho}$ is the density-based selectivity and G the field strength expressed as acceleration [24]. If neither G nor $\Delta\rho$ vary, then the corresponding term on the right-hand-side of Eq. 9 can be included with log t_{R1} into a final constant log t_n [23]:

$$\log t_n = S_{\Delta\rho}\log G\Delta\rho + \log t_{R1} \quad (11)$$

When a sample has a different density (i.e., a different $\Delta\rho$) from that of the latex calibrant, it can be made to migrate inside the channel at the same velocity as the latex standards, thus compensating for the change in density, the primary driving force remaining the same. This is accomplished by changing the field strength of the centrifuge so that the change in density is exactly offset by the change in rpm [16]. The adjustment in rpm making the product $G\Delta\rho$ equal for the sample and calibrant enables direct use of the latex calibration curve, provided that the sample particles have the same density [16].

From the experimental calibration parameters, $-S_{ds}$ and t_n, the particle size distribution $p(d)$ is obtained according to equation [16]:

$$p(d) = c(t_R)\dot{V}S_d t_n\left(\frac{t_R}{t_n}\right)^{(S_d+1)/S_d} \quad (12)$$

where $c(t_R)$ is the detector signal, $\dot{V}$ the volumetric flow-rate. If the detector at the end of the FFF channel provides a signal proportional to particle mass, then a mass distribution curve is provided by modifying Eq. 12:

$$p(d) = c(t_R)d^{\omega}\dot{V}S_d t_n\left(\frac{t_R}{t_n}\right)^{(S_d+1)/S_d} \quad (13)$$

where the optical weighting constant ω is 1 for the mass distribution [17].

3. Experimental

The SPLITT cell used in this study is a Model SF1000HC (FFFractionation, Salt Lake City, UT, USA). The channel thickness is 380 μm and defined by the combined thickness of two mylar spacers and one stainless steel sheet spacer. All these components were sandwiched between two 45.8×5×0.5 cm glass pieces, forming the upper and lower walls of the channel. The other cell dimensions are the length $L=20$ cm and the width of the stainless steel splitter $b=4$ cm. The geometric volume of the cell is then 3.04 ml. Two Plexiglas blocks bolted the above-mentioned assorted layers together. Two sheets of PTFE were inserted between the Plexiglas and the glass blocks to prevent the glass blocks from breaking.

Two peristaltic pumps, Minitan (Millipore, Vimodrone, Italy) and Minipuls3 (Gilson, Middleton, WI, USA), were employed to provide independent flow streams to inlets a′ and b′. The flow-rates at the outlets were controlled by using proper standard tubing of different lengths and diameters. The SPLITT cell was used in the so called ''transport mode'', where the diffusion mechanisms are not relevant [4,8,18]. The experimental conditions used for each separation are summarized in Tables 1 and 2.

A commercial wheat starch sample, with a measured granule density of 1.498 g/ml, was separated with the SPLITT cell, respectively, as 0.070%, 0.125%, 0.250% and 0.500% (w/v) suspension, dispersed in Milli-Q water (Millipore, Bedford, MA,

Table 1
Experimental conditions for the starch SPLITT separations

$d_{c,\ theor}$ (μm)	$\Delta\dot{V}_{theor}$ (ml/min)	Volumetric flow-rate (ml/min)				$\Delta\dot{V}^{a}_{real}$ (ml/min)	$w_{a'}$ (μm)	w_t (μm)	$d_{c,\ exp}$ (μm)
		a′	b′	a	b				
15	27.0	1.0	28.0	26.5	2.5	25.5	42.34	268.97	14
8	7.0	1.0	8.0	7.8	1.2	6.8	78.78	214.19	7
3	1.0	3.0	4.0	4.1	2.9	1.1	171.84	39.96	3

[a] $\Delta\dot{V}_{real}$ is the effective, experimental $\Delta\dot{V}$ realized inside of the SPLITT cell. Its values are close to, but not coincident with, the theoretical values ($\Delta\dot{V}_{theor}$). The correspondent real cut-off diameters are reported in the last column.

USA) or a 0.1% (v/v) FL70 solution or a 0.05% (v/v) Triton X-100 solution; (see Tables 1 and 2 for the experimental details and Fig. 2 for optical photographs of the separation results).

The SdFFF apparatus is a Model S101 (FFFractionation) with channel walls made of hastelloy C. The channel, cut from a mylar spacer of nominal thickness 0.0250 cm, has a void volume of 4.6 ml. The instrument was calibrated to work under steric conditions using polystyrene samples of density of 1.05 g/ml and certified diameter (2.05, 2.91, 6.125, 10.527, 21.7, 24.3 μm; Polyscience, Warrington, PA, USA). Different centrifuge fields were applied (see Table 3) while the flow-rate was always 10 ml/min, generated by an HPLC pump Model 422 Master (Kontron Instruments, Italy). Two different carriers

Table 2
Experimental conditions for the SPLITT separations[a]

	Concentration (%, w/v)	$\dot{V}$(a′) (ml/min)	$\dot{V}$(b′) (ml/min)	$\dot{V}$(a) (ml/min)	$\dot{V}$(b) (ml/min)	$\dot{V}$ (ml/min)	$\frac{\dot{V}(a')}{\dot{V}(t)}$	$\frac{\dot{V}(b')}{\dot{V}(t)}$	$w_{a'}$ (μm)	w_t (μm)
1a	0.070	1	15.1	15.0	1.1	16.1	0.07	1.02	57.67	261.66
2a		2	14.9	15.7	1.2	16.9	0.14	1.09	81.53	236.55
3a		2	16.0	16.0	2.0	18.0	0.14	1.14	78.78	222.45
4a		3	16.1	17.0	2.1	19.1	0.21	1.15	95.28	206.40
5a		4	16.2	18.0	2.2	20.2	0.29	1.16	108.50	193.57
6a		5	16.0	18.7	2.3	21.0	0.36	1.17	120.56	181.28
1b	0.125	1	15.1	15.0	1.1	16.1	0.07	1.02	57.67	261.66
2b		2	15.2	16.0	1.2	17.2	0.14	1.08	80.75	235.90
3b		2	16.0	16.0	2.0	18.0	0.14	1.14	78.78	222.45
4b		3	16.0	16.7	2.3	19.0	0.22	1.17	95.55	201.90
5b		4	16.0	17.7	2.3	20.0	0.29	1.17	109.11	190.62
6b		5	16.0	18.7	2.3	21.0	0.36	1.17	120.56	181.28
1c	0.250	1	15.1	15.0	1.1	16.1	0.07	1.02	57.67	261.66
2c		2	15.2	16.0	1.2	17.2	0.14	1.08	80.75	235.90
3c		2	16.0	16.0	2.0	18.0	0.14	1.14	78.78	222.45
4c		3	16.1	17.0	2.1	19.1	0.21	1.15	95.28	206.40
5c		4	16.0	17.7	2.3	20.0	0.29	1.17	109.11	190.62
6c		5	16.0	18.7	2.3	21.0	0.36	1.17	120.56	181.28
1d	0.500	1	15.0	15.2	0.8	16.0	0.07	1.05	57.86	270.70
2d		2	15.2	16.3	0.9	17.2	0.14	1.06	80.75	246.57
3d		2	16.0	16.0	2.0	18.0	0.14	1.14	78.78	222.45
4d		3	16.1	17.0	2.1	19.1	0.21	1.15	95.28	206.40
5d		4	16.2	18.0	2.2	20.2	0.28	1.16	108.50	193.57
6d		5	16.0	18.7	2.3	21.0	0.36	1.17	120.56	181.28

[a] Theoretical diameter cut-off $d_c = 10$ μm, $\Delta\dot{V} \approx 14$ ml/min, $w = 380$ μm.

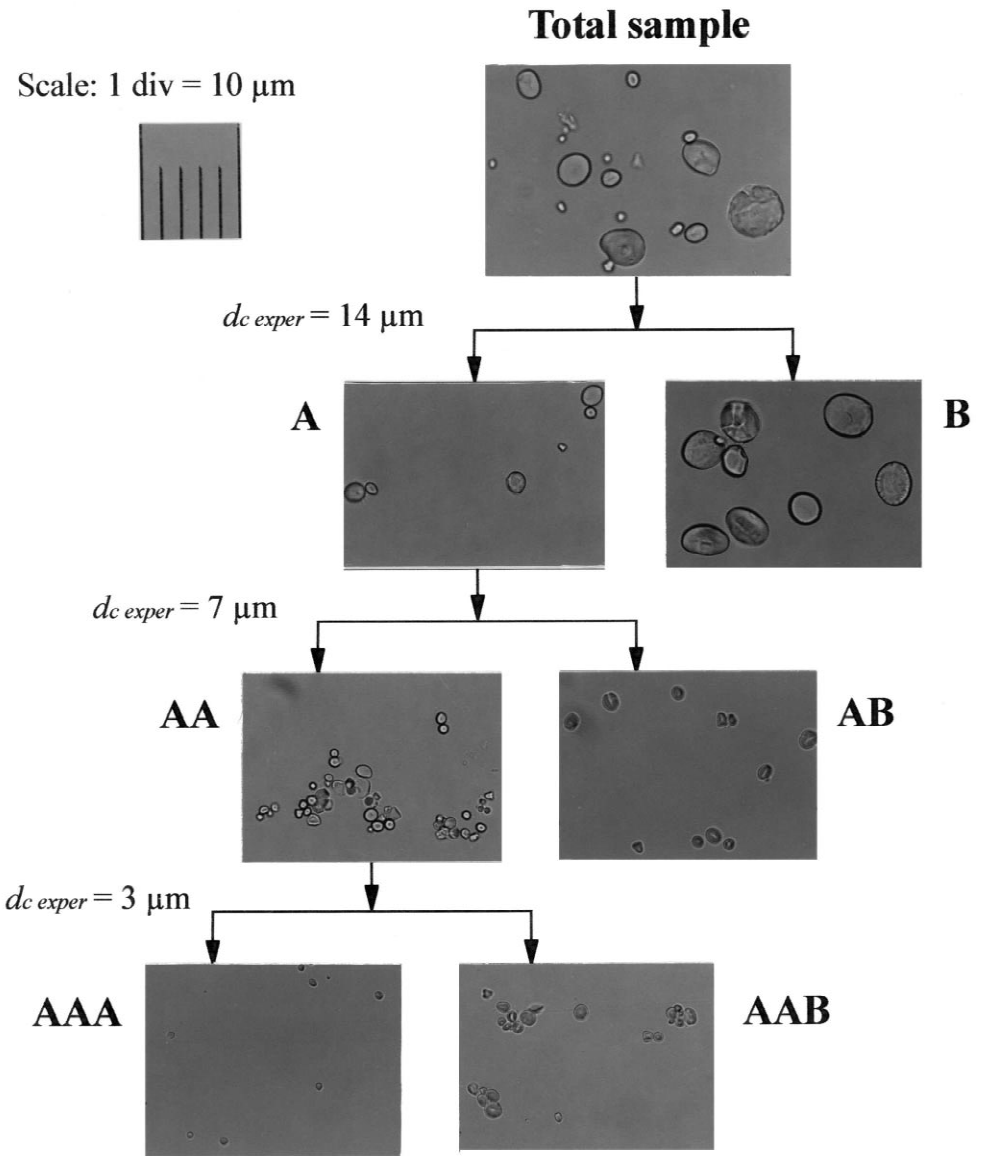

Fig. 2. SPLITT cell separation of the starch sample: scheme and optical photographs of the fractions. The separation d_c values were: 14, 7 and 3 μm. The granules were suspended in Milli-Q water and no surfactant was added to the carrier.

Table 3
Experimental conditions for the Sd/StFFF calibration

Carrier	0.1% (v/v) FL70 + 0.02% (w/v) NaN_3			0.05% (v/v) Triton + 0.01% (w/v) NaN_3		
Field	500 rpm	600 rpm	700 rpm	700 rpm	900 rpm	1025 rpm
S_d	−0.898±0.069	−0.889±0.063	−0.876±0.057	−0.856±0.051	−0.878±0.058	−0.911±0.048
Log t_n	1.731±0.067	1.756±0.062	1.765±0.056	1.709±0.049	1.784±0.062	1.844±0.050
R	0.988	0.990	0.991	0.993	0.993	0.996

Table 4
Conditions for the Sd/StFFF starch separations

Field type	Initial field (rpm)	Stop flow (min)	Run field (rpm)	Flow-rate (ml/min)	$G\Delta\rho$ (g/ml)
Constant	325	2	325	10	8.84
Constant	220	2	220	10	4.12

were used: (1) a solution of 0.02% (w/v) NaN_3 (bactericide) and 0.1% (v/v) FL70 (dispersing agent); (2) 0.01% (w/v) NaN_3 and 0.05% (v/v) Triton X-100 (dispersing agent) (Sigma–Aldrich, Germany). The system outlet tube was connected to a UV detector operating at 254 or 330 nm (Uvidec 100, Jasco, Japan). The signal $c(t_R)$ was fed to a Linseis Model L 6512 X–Y recorder (Linsel, Germany). Signal data were also collected by an ACRO-900 12 bit I/O acquisition system (Acrosystems, Beverly, MS, USA).

The Sd/StFFF experimental conditions for the starch separation are reported in Table 4. Starch samples, coming from SPLITT separations, were injected with volumes ranging from 50–100 μl, after a concentration step (ratio 1:200) performed on the total volumes processed. Narrow SdFFF fractions of eluted starch were collected using a 2110 Bio-Rad fraction collector (Bio-Rad Labs., Richmond, CA, USA) and were examined by an optical microscope after concentration on 0.1-μm pore polycarbonate etched-track membrane Nucleopore filters. Some results are shown in Fig. 7.

4. Discussion

4.1. Carrier composition

The particle size distribution of the considered starch sample, containing both small (≈2 μm) and large particles (up to 55 μm), is very broad. For such samples a two-step run is generally recommended: the first to remove the very large particles under high flow-rate conditions; the second to perform the desired operation on the remaining particles [25]. Each experimental run was adjusted to achieve a binary fractionation at around a designated cut-off diameter of 50%; that is, where half of the particles exit through outlet a and the other half through outlet b. Three different diameter cut-offs were selected: 15, 8, 3 μm and the correspondent SPLITT cell separation conditions are reported in Table 1. This first separation set was performed using only Milli-Q water for both the carrier and as dispersing medium for the starch granules. Each separation step was repeated twice without altering the set flow-rates. To prevent sample contamination by extraneous substances and to make the subsequent washing steps unnecessary, no surfactant was used for these separations. The final fractions obtained from the SPLITT treatment are shown in Fig. 2 (optical photographs). The results are satisfactory if one compares the sizes of the photographed particles with the reported scale.

It has to be underlined that for this kind of sample, the computed diameters refer to dry granules and, because of the swelling, may not coincide with those of the wet granules.

The main drawbacks of this procedure used without surfactants were: the formation of difficult to remove air bubbles inside of the cell and the depositing of granules on the lower cell wall. Specific interactions [26] between the starch granules and the cell constituent materials appeared only to be amplified when Milli-Q water was used. A further investigation of this point would require systematic investigation of the medium composition effect (e.g., ionic strength effects) which, at the moment, lies beyond the aim of the present study.

In order to overcome the above-mentioned drawbacks, two different surfactants were considered: FL70 and Triton X-100. When the results of SPLITT separation and the Sd/StFFF runs were compared, no significant differences in separation performance were found. In the light of this evidence Triton X-100 was preferred because its more commonly used.

By using surfactants, reducing the surface tension of the aqueous medium and the particle–wall interac-

tions [27,28], the inlet splitter and the lower wall of the cell were kept perfectly clean during all the experiments. Unfortunately, the interaction between these organic substances and the granule surface is irreversible and this can be a serious drawback for the subsequent employment of the fractionated starch sample.

4.2. Flow-rates and sample concentration effects

Since the performance of the SPLITT cell is strictly related to the choice of the four flow-rates and to the concentration of the sample feed stream [20], a study was undertaken to investigate how these two aspects act on this sample. A cut-off diameter of 10 μm was selected and Eq. 6 was used to compute $\Delta\dot{V}=14$ ml/min. Table 2 reports the different concentrations and the different flow-rates applied for this study. The main purpose of this study was to single out the combination of experimental conditions (concentration–flow-rates) able to produce a fraction containing mainly particles with sizes smaller than the set cut-off diameter without a preliminary cleaning of the parent sample. Once these conditions are identified, the next step is to perform the separation twice under the same conditions.

Using the data reported in Table 2, we can compute the values of the ratios $\dot{V}(a')/\dot{V}(t)$, governing the inlet feed of the cell, and $\dot{V}(b')/\dot{V}(t)$, regulating dilution of the sample inside of the cell. It is worth noting that they always fall within the suggested ranges (0.1–0.3 and 1.5–3.0, respectively) and this should assure good separation resolution [7]. The same Table also reports the w_t values of the transport region thickness (column 10). These values were computed using the following equation [29]:

$$w_t = w_a - w_{a'} \quad (13)$$

where $w_{a'}$, the distance of the ISP from wall A (see Fig. 1), is given by the ratio $\dot{V}(a')/\dot{V}$ [5,29], with $\dot{V}$ being the total volumetric flow-rate; in like manner w_a, the distance of the outer surface plane (OSP) from wall A, is given by the ratio $\dot{V}(a)/\dot{V}$. The worst case corresponds to the highest flow-rates, for which only 48% of the total cell thickness is available for the gravitational field-induced separation. On the outset this condition appears to be a disadvantage but one must remember that separation inside the SPLITT channel is the result of a combination of several effects. Therefore, even under these apparently limited conditions, the separation can prove good thanks to the contribution of other dynamic effects, such as lift forces, which have been neglected in this theoretical treatment but which, under high flow-rate conditions, can strongly affect the final separation results of such large particles.

Fig. 3a shows the percentage of granules up to 10 μm in size seen in fractions A as a function of the inlet flow-rate $\dot{V}(a')$. The percentage was computed

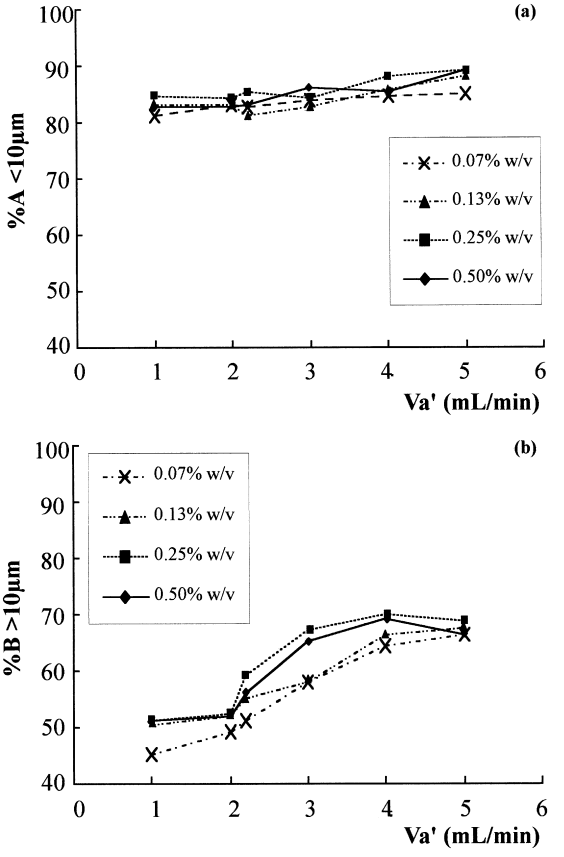

Fig. 3. (a) Measured concentrations of the starch granules of the SPLITT fractions A with $d_c<10$ μm as a function of the inlet volumetric flow-rate $\dot{V}(a')$. (b) Measured concentrations of the starch granules of the SPLITT fractions B with $d_c>10$ μm as a function of the inlet volumetric flow-rate $\dot{V}(a')$. Each symbol corresponds to a different feed sample concentration: × 0.07% (w/v), ▲ 0.13% (w/v), ■ 0.25% (w/v) and ♦ 0.50% (w/v).

by counting, under an optical microscope, the granules present in the concentrated fractions A. The number of granules counted in each fraction averaged 1000. Recovery of the small granules was always greater than 80%, with a slow increase toward the highest inlet flow-rates. In general, the best recoveries were obtained in correspondence of $\dot{V}(a')=4$ or 5 ml/min. An analogous investigation was carried out on all fractions B, and the results are reported in Fig. 3b. In this case the best recoveries were found at the highest flow-rates, confirming, and indeed reinforcing, the previous results: a change from around 50% [$\dot{V}(a')=1$–2 ml/min] to 70% [$\dot{V}(a')=4$–5 ml/min] compared to a change from around 80% [$\dot{V}(a')=1$–2 ml/min] to 90% [$\dot{V}(a')=$ 4–5 ml/min] found for fractions A.

The second part of study aimed at singling out the most appropriate sample concentration for the SPLITT separation. The quantity of particles smaller than the set d_c (10 μm) were counted in fractions A and the results plotted as a function of the tested feed stream concentrations. Fig. 4a shows the trend in these percentages. Concentration did not have one unique effect on all the inlet flow-rates investigated; however, for the highest $\dot{V}(a')$ values considered, the best recovery was achieved at a 0.25% (w/v) concentration. This concentration lies between the two different starch concentrations (0.1% and 1%, w/v) previously reported in literature [7]; however, no systematic investigation on the effect of concentration was performed in these previous works. Looking at fractions B, reported in Fig. 4b, a different trend can be observed. The concentration of granules greater than 10 μm is almost constant at around 51% for $\dot{V}(a')=1$ and 2 ml/min, and 67% for $\dot{V}(a')=4$ and 5 ml/min. An intermediate situation is observed for $\dot{V}(a')=2$ and $\dot{V}(b')=15$ ml/min, and $\dot{V}(a')=3$ ml/min, for which the highest recovery is found at the 0.25% (w/v) concentration.

The obtained results are also in agreement with those presented by Jiang et al. [20], who analyzed different samples, silica ($\rho_p=2.5$ g/ml and cut-off diameter $d_c=14$ μm) and diamond ($\rho_p=3.5$ g/ml with $d_c=4$ μm). They found that smaller particles or lower-density particles usually require preparation and separation at a lower concentration. In our case the starch granules have a density lower than the silica particles, and the $d_c=10$ μm is close to $d_c=14$ μm. Therefore, the concentration able to ensure acceptable resolution, found at 0.25% (w/v), is accordingly lower than the 1–2% found for the silica particles. This value is also close to what was singled out for diamond particles where a much lower d_c was set [20].

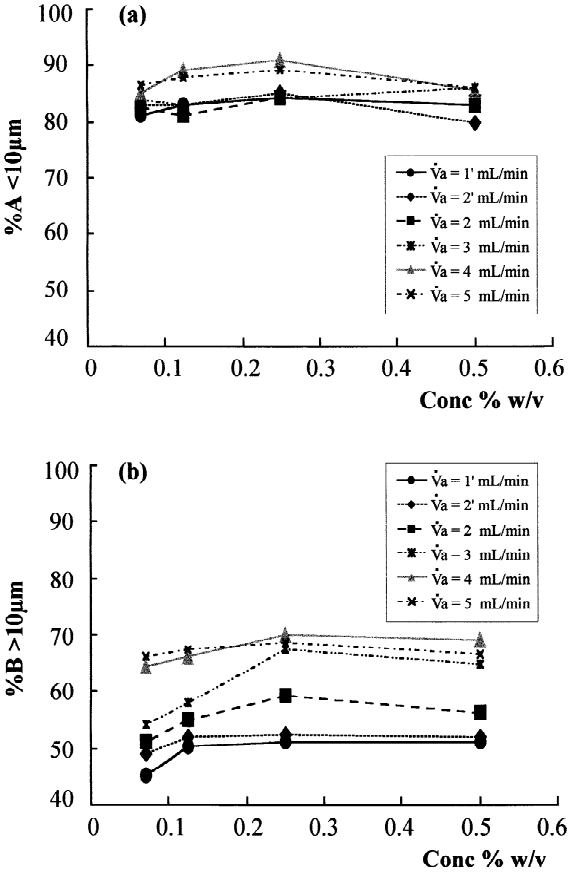

Fig. 4. (a) Measured concentrations of the starch granules of the SPLITT fraction A with $d_c<10$ μm as a function of the concentration of the inlet feed flow-rate $\dot{V}(a')$. (b) Measured concentrations of the starch granules of the SPLITT fractions B with $d_c>10$ μm as a function of the concentration of the inlet feed flow-rate $\dot{V}(a')$. Prime (′) indicates the separations obtained with $\dot{V}(b')=15$ ml/min.

What appears evident from these studies is that there is not one single critical concentration for all samples; rather this concentration must be determined according to particle size range and density. The explanation for this lies in the different density between the top feed stream and the bottom particle-free carrier stream [20]. In fact, it is known that, as

the density of the feed stream becomes somewhat higher than the density of the carrier stream, significant mixing of oversized and undersized particles occurs in the SF channel. Consequently, particles of all sizes (present in the original sample) exit from both outlets a and b, and separation is poor for almost all ranges of particles sizes [19]. In our case the density of the substream a′, should not be so high as to cause a significant mixing between the two substream a and b; rather the contamination of the a fraction with the larger particles can be justified by admitting that the larger particles, belonging to the denser stream running close to the upper wall, tend to settle through the cell (at least remaining in the denser region) more slowly than they would in a isopicnic medium. Consequently these particles will emerge through the upper exit It is also true that the d_c value is set at about 1/6 of highest starch granule diameter while there is evidence that the lowest contamination between the fraction occurs when the cut-off diameter is chosen close to the center of the distribution, especially if attention is turned to the oversized particles [7].

Under the established experimental conditions, a new SPLITT separation was performed, by setting the feed sample concentration to 0.25% (w/v), the cut-off diameter $d_c = 10$ μm, $\dot{V}(a') = 4$ ml/min, $\dot{V}(b') = 15.9$ ml/min, $\dot{V}(a) = 17.7$ ml/min and $\dot{V}(b) = 2.2$ ml/min. The fraction B was collected and dried under an IR lamp, keeping the temperature under control (≤25°C) to avoid any chemical modification of the starch particles (e.g., surface hydrolysis). The dried sample was dispersed in the carrier solution to make up a new 0.25% (w/v) suspension and the second separation was performed under the same flow-rate conditions. The final results are reported in Fig. 5. Fractions A and B were then used as samples for the Sd/StFFF characterization.

4.3. Sd/steric FFF characterization

The feasibility of using the steric FFF technique as a convenient monitoring system for particle size distributions of SPLITT fractions is well known. In order to obtain useful Sd/StFFF results for the size distribution, an empirical calibration curve must be

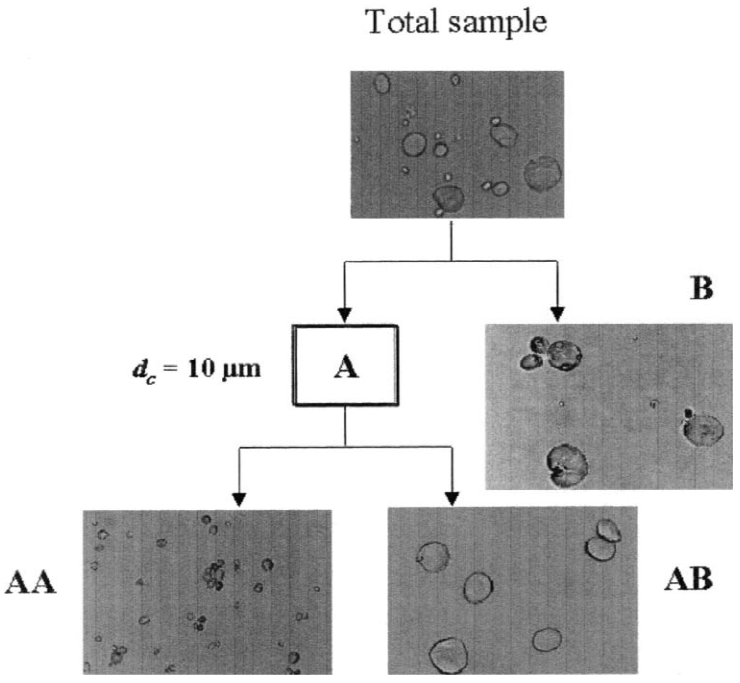

Fig. 5. SPLITT cell separation of the starch sample performed with the feed sample concentration of 2.5% (w/v), $d_c = 10$ μm, $\dot{V}(a') = 4$ ml/min, $\dot{V}(b') = 15.9$ ml/min, $\dot{V}(a) = 17.7$ ml/min and $\dot{V}(b) = 2.2$ ml/min. Scheme and optical photographs of the fractions.

constructed and those computed in this study are shown in Fig. 6. Two series of calibration plots were obtained at different field conditions: one using a solution of FL70, already used as a carrier for starch separations [17] and the other using Triton X-100 in order to test whether this surfactant affects the separation and/or improves the UV detection. The result shows a sheaf of straight lines, with different intercept values depending on the field conditions. The average t_n parameter (i.e., the extrapolated retention time for a 1 μm particle) obtained from the lines is 58 min. No significant variations in the S_d values were found when the surfactant was changed.

Once the calibration of the Sd/StFFF was completed, the starch SPLITT fractions were analyzed by applying the density compensation procedure. The separations were obtained at 325 rpm, corresponding

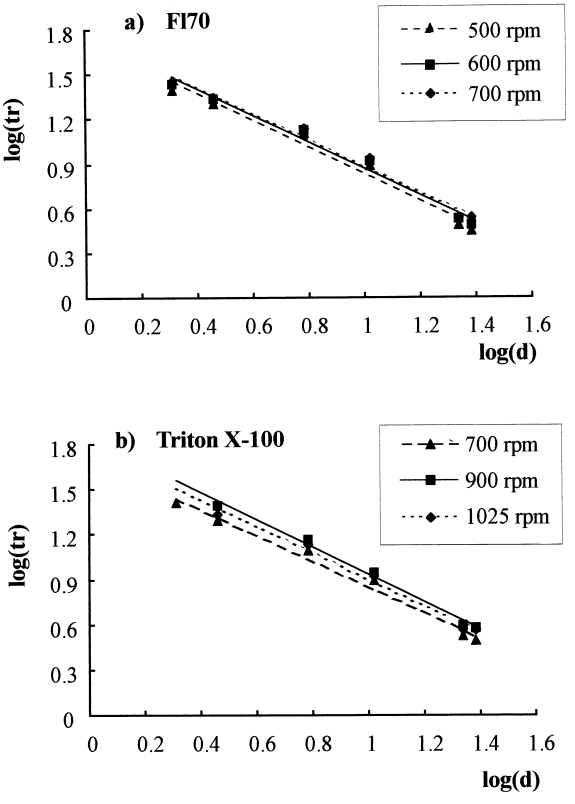

Fig. 6. Sd/StFFF calibration curves obtained by using standard polystyrene samples; PS diameters = 2.05, 2.91, 6.125, 10.527, 21.7 and 24.3 μm and different surfactants: (a) FL70 and (b) Triton X-100 (see Table 3 for other experimental conditions).

to 17.76 gravities, either in FL70 and Triton X-100. The starch granules had the same behavior in both carriers: the measured density, retention times and apparently also the optical UV detection properties were always the same. A more detailed investigation exploring this point lies beyond the aim of the present paper.

The starch samples here considered are: (1) a pair of fractions A and B ($d_c = 8$ μm) separated by SPLITT only once and only in Milli-Q water; and (2) the SPLITT fractions AA and AB ($d_c = 10$ μm), separated twice in Triton X-100 under the previously described experimental conditions.

Fig. 7 reports the particle size distributions of the SPLITT fractions A and B ($d_c = 8$ μm). The optical microscope observation of the collected fractions proves that the SdFFF was well calibrated and that the chosen experimental conditions give a good Sd/StFFF separation. The real dimensions of the particles, collected in the SdFFF fractions and photographed at the optical microscope, appear to correspond well with those computed by the calibration curve. What stands out as evidently wrong in this figure is that the SPLITT separation produced two poorly resolved fractions. This confirms that this kind of sample cannot undergo a single SPLITT separation and that the use of some surfactant as dispersing agent in the aqueous medium is strongly recommended.

Fig. 8a and b show, on the other hand, the UV response as a function, respectively, of the particle diameter and the particle size distribution of the separation of the second pair of SPLITT fractions: AA and AB, obtained in Triton X-100 by a double step SPLITT separation. In this case the SPLITT separation produced two well resolved fractions. Here no SdFFF fraction was collected as Sd/StFFF performance had already been proven for such samples. The two peaks overlap at around 10 μm, as expected by the SPLITT conditions applied.

As supplementary test a Sd/StFFF separation was performed at 220 rpm (8.28 = gravities) to determine whether the strength of the applied centrifugal field could be decreased, thus reducing granule–channel wall interactions. Unfortunately, although the corresponding polystyrene calibration plot suggests a possible analysis, optical microscope inspection of some of the collected fractions showed that the

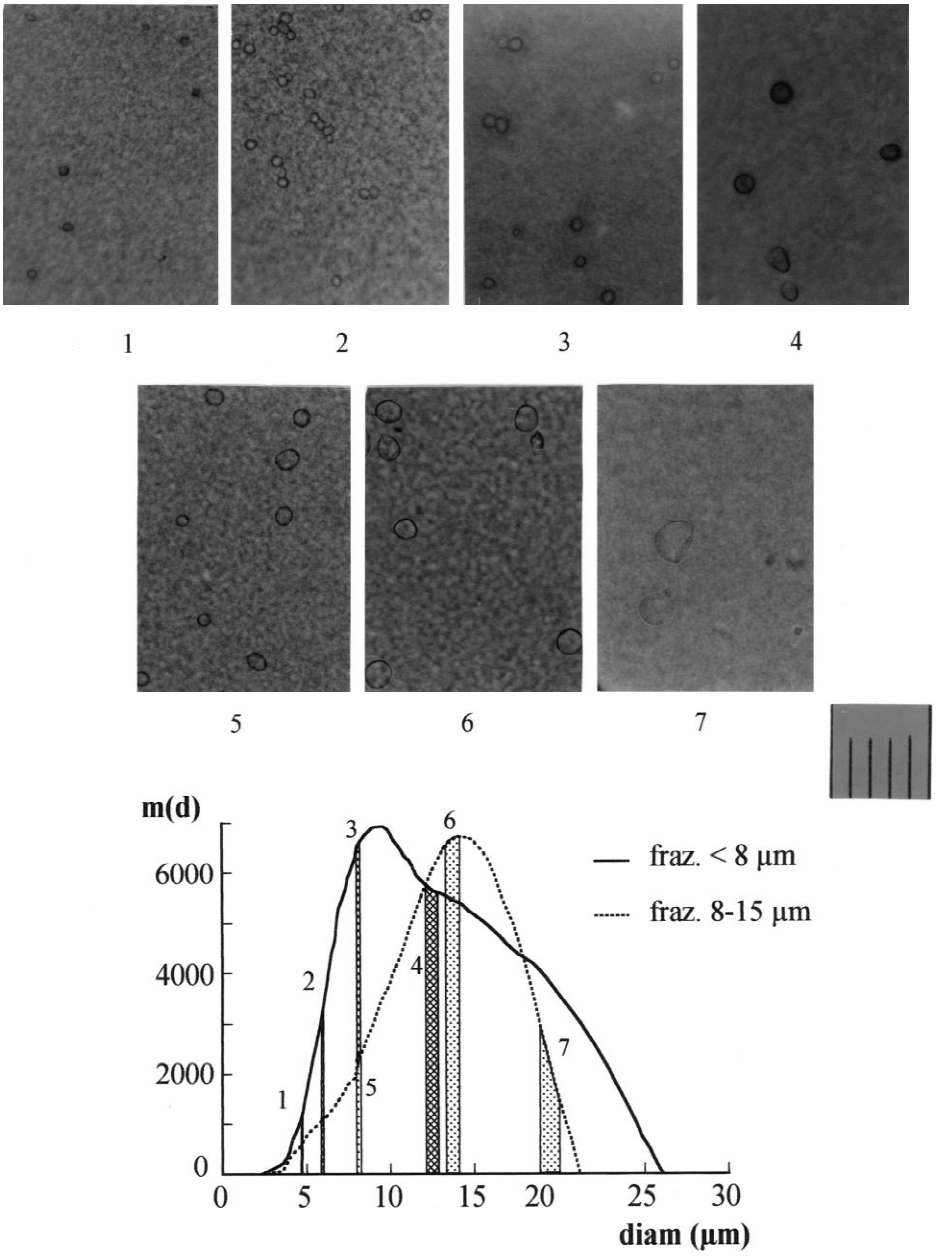

Fig. 7. Sd/StFFF particle size distributions and optical photographs of two SPLITT fractions separated by using only Milli-Q water [see Table 1 for the SPLITT conditions and Table 4 for the Sd/StFFF conditions: (constant field=325 rpm)]. ''Fraz'' means fraction.

separation had occurred through a mixed mechanism: normal and steric [30]. This last experimental evidence also confirms that choice of the SdFFF field strength used in separating the real sample is indeed a critical parameter.

5. Symbols

b	Width of the SPLITT channel
d	Particle diameter
d_c	Cut-off diameter

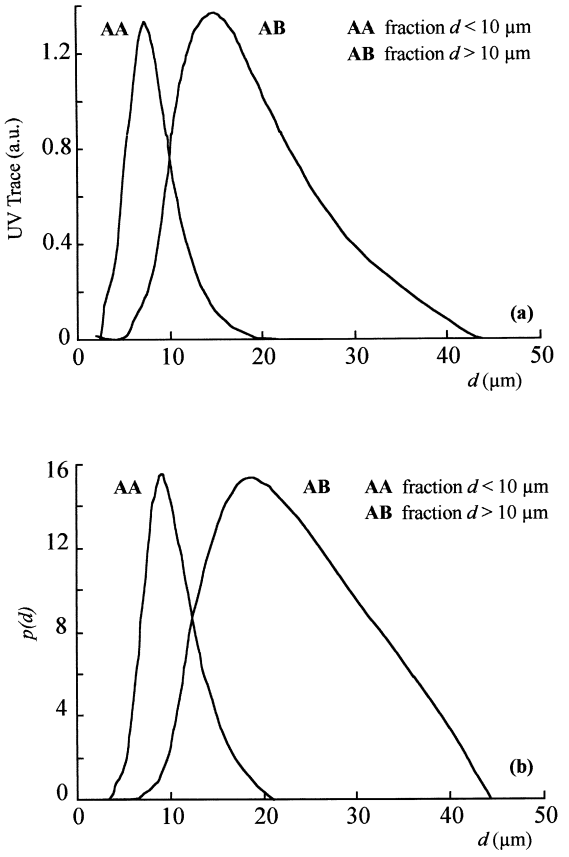

Fig. 8. (a) Sd/StFFF UV trace as a function of the particle diameter for the AA and AB (d_c = 10 μm) SPLITT fractions; (b) particle size distributions of the same fractions. [Carrier = 0.05% (v/v) Triton X-100 + 0.01% (w/v) NaN_3; Sd/StFFF conditions are reported in Table 4 – constant field = 325 rpm].

G	Gravity acceleration
L	Length of the SPLITT channel
t_R	Retention time
t_n	Known linear calibration plot parameter
S_{ds}	Diameter-based selectivity
U	Particle migration velocity
$\dot{V}$	Total volumetric flow-rate through cell
$\dot{V}(a')$	Volumetric flow-rate at outlet a′
$\dot{V}(b')$	Volumetric flow-rate at outlet b′
$\dot{V}(a)$	Volumetric flow-rate at inlet a
$\dot{V}(b)$	Volumetric flow-rate at inlet b
$\dot{V}(t)$	Volumetric flow-rate of the transport region
$\Delta\dot{V}$	Volumetric flow-rate across the cell and perpendicular to bL plane
w	Total thickness of the SPLITT cell
w_a	Thickness of the outlet upper stream
$w_{a'}$	Thickness of the inlet upper stream
w_t	Thickness of the transport region
η	Carrier viscosity
ρ_l	Carrier density
ρ_p	Particle density

Acknowledgements

This work was financially supported by the European Commission Contract No. ERB IC15-CT98-0909, by the Italian Research Council (CNR) and by the Italian Ministry of the University and Scientific Technological Research (MURST, 60% and 40%). The authors thank the staff of the Department of Evolutive Biology for use of the Optical Microscope.

References

[1] R. Hanselmann, W. Burchard, M. Ehrat, H.M. Widmer, Macromolecules 29 (1996) 3277.
[2] J.-L. Jane, in: P.J. Frazier, A.M. Donald, P. Richmond (Eds.), Starch – Structure and Functionality, The Royal Society of Chemistry, 1997, p. 27.
[3] R. Whistler, J.N. BeMiller, E.F. Paschall, Starch – Chemistry and Technology, Academic Press, New York, 1984.
[4] C. Contado, F. Dondi, R. Beckett, J.C. Giddings, Anal. Chim. Acta 345 (1997) 99.
[5] P.S. Williams, S. Levin, T. Lenczycki, J.C. Giddings, Ind. Eng. Chem. Res. 31 (1992) 2172.
[6] S. Levin, G. Tawil, Anal. Chem. 65 (1993) 2254.
[7] C.B. Fuh, M.N. Myers, J.C. Giddings, Anal. Biochem. 64 (1992) 3125.
[8] S.R. Springston, M.N. Myers, J.C. Giddings, Anal. Chem. 59 (1987) 344.
[9] Y. Gao, M.N. Myers, B.N. Barman, J.C. Giddings, Part. Sci. Technol. 9 (1991) 105.
[10] C.B. Fuh, M.N. Myers, J.C. Giddings, Ind. Eng. Chem. Res. 33 (1994) 355.
[11] R. Keil, E. Tsamakis, C.B. Fuh, J.C. Giddings, J.I. Hedges, Geochim. Cosmochim. Acta 58 (1994) 879.
[12] C.B. Fuh, J.C. Giddings, Biotechnol. Prog. 11 (1995) 14.
[13] J.C. Giddings, Sep. Sci. Technol. 23 (1988) 931.
[14] S. Levin, M.N. Myers, J.C. Giddings, Sep. Sci. Technol. 24 (1989) 1245.
[15] S. Levin, J.C. Giddings, J. Chem. Soc. Tech. Biotechnol. 50 (1991) 43.
[16] J.C. Giddings, M.H. Moon, P.S. Williams, N.M. Myers, Anal. Chem. 63 (1991) 1366.
[17] M.H. Moon, J.C. Giddings, J. Food Sci. 58 (1993) 1166.

[18] F. Dondi, C. Contado, G. Blo, S. Garçia Martin, Chromatographia 48 (1998) 643.
[19] S. Gupta, S.P. Lingrani, J.C. Giddings, Sep. Sci Technol. 32 (10) (1997) 1629.
[20] Y. Jiang, A. Kummerow, M. Hansen, J. Microcol. Sep. 9 (1997) 261.
[21] J.C. Giddings, Sep. Sci. Technol. 27 (1992) 1489.
[22] J.C. Giddings, X. Chen, K.G. Wahlund, K.D. Caldwell, M.N. Myers, Anal. Chem. 53 (1987) 1957.
[23] J.C. Giddings, S.K. Ratanathanawongs, M.H. Moon, KONA: Powder Particle 9 (1991) 200.
[24] S.R. Springston, M.N. Myers, J.C. Giddings, Anal. Chem. 64 (1992) 3125.
[25] Instrument Manual for Series SF1000 SPLITT Particle Separator, FFFractionation Ltd, Salt Lake City, UT, 1997, Version 1.
[26] Y. Mori, K. Kimura, M. Tanigaki, Anal. Chem. 62 (1989) 2668.
[27] M. Hansen, J.C. Giddings, Anal. Chem. 61 (1989) 811.
[28] Y. Mori, B. Scarlett, H.G. Merkus, J. Chromatogr. 515 (1990) 27.
[29] J. Zhang, P.S. Williams, M.N. Myers, J.C. Giddings, Sep. Sci. Technol. 29 (1994) 2493.
[30] S. Lee, J.C. Giddings, Anal. Chem. 60 (1988) 2328.